Momentum-resolved Raman spectroscopy of a noninteracting ultracold Fermi gas

Pengjun Wang, Zhengkun Fu, Lianghui Huang, and Jing Zhang*

State Key Laboratory of Quantum Optics and Quantum Optics Devices, Institute of Opto-Electronics, Shanxi University, Taiyuan 030006, People's Republic of China

(Received 6 April 2012; published 18 May 2012)

We report the experiment on probing the one-body spectral function in a trapped noninteracting ^{40}K Fermi gas by means of the momentum-resolved Raman spectroscopy. The experimental result is in good agreement with the expected quadratic dispersion in the noninteracting regime. Through the comparison with the radio-frequency spectrum, we found that the Raman spectrum shows some new characteristics.

DOI: 10.1103/PhysRevA.85.053626 PACS number(s): 67.85.Lm, 03.75.Ss

During the past decade, the remarkable advances in the study of ultracold atomic gases have promoted the birth to many interesting research fields. As an interacting quantum system with highly tunable parameters, it offers us new opportunities to efficiently simulate quantum condensed matter systems. The observation of superfluidity of Fermi gases [1–3], the pairing gap and pseudogap behavior [4,5], the quantum simulation of quantum magnetism and antiferromagnetic spin chains in an optical lattice [6,7] and the generation of synthetic gauge fields of bosons [8–11] and fermions [12] were considered to be the important milestones in this field. In the context of the strongly interacting fermionic atoms at the vicinity of the Feshbach resonance, the crossover from the Bardeen-Cooper-Schrieffer (BCS) superfluid state to the Bose-Einstein-condensate (BEC) superfluid state [13–15] has attracted a lot of attention. Many tools have been proposed and used to study the strongly interacting atomic Fermi gases, for example, spatial noise correlations [7,16], radio-frequency (RF) spectroscopy [4,5,17–21], momentum-resolved stimulated Raman technique [22,23], and Bragg spectroscopy [24,25].

RF spectroscopy technology as a simple and valuable tool has been used for experimentally studying physical properties of fermionic ultracold atoms, such as to decide the scattering length near a Feshbach resonance by directly measuring the RF shift induced by mean-field energy [17], to demonstrate the quantum unitarity and many-body effect [18], to probe the occupied density of single-particle states and energy dispersion through BEC-BCS crossover [5], and to explore the strongly interacting two-dimensional Fermi gas [26–29]. Besides RF spectroscopy, Raman spectroscopy is also an important tool. In fact, RF spectroscopy can be regarded as a special case of Raman spectroscopy with a vanishing transferred momentum. In the stimulated Raman process, atoms are transferred into a different internal state by absorbing a photon from a laser beam and immediately reemitting the absorbed photon into another laser beam with different frequency and wave vector. Raman spectroscopy has several significant advantages comparing with RF spectroscopy [23], that are their spatial selectivity to eliminate inhomogeneous broadening due to the trap potential, tunability of the transferred momentum from below to well above the Fermi momentum, and weaker sensitivity to final-state interactions. The theoretical studies on utilizing Raman spectroscopy to probe the excitation spectrum of strongly correlated phases of Bose gases confined to optical lattices [30,31], to detect the energy structure of bosonic atoms in a 1D lattice [32] and to investigate single-particle excitations in normal and superfluid phases of strong interacting Fermi gases [22,23] have been accomplished. However, the corresponding experimental demonstration has not been presented so far.

In this paper, we report an experimental study on the momentum-resolved Raman spectroscopy of an ultracold noninteracting Fermi gas, in which the single-particle excitation is probed. The quadratic dispersion in the noninteracting regime of Fermi gas is obtained with Raman spectroscopy technique. Comparing with the RF spectrum, we found the several advantages of Raman spectroscopy. This detection technology can be easily extended to probe the characteristics of Fermi gas in the strongly interacting regime.

The Raman process is sketched in Figs. 1(a) and 1(b). The atoms in the initial hyperfine state $|\uparrow\rangle$ are transferred into the final empty state $|\downarrow\rangle$ by absorbing a photon from the laser beam 1 with frequency ω_1, wave vector $\mathbf{k}_1$, and Rabi frequencies Ω_1 and then immediately emitting a photon into another laser beam 2 with frequency ω_2, wave vector $\mathbf{k}_2$, and Rabi frequencies Ω_2. The two laser fields are far detuned Δ from resonances with the intermediated excited state so that the spontaneous emission can be neglected. The effective Raman coupling of Raman process is defined as $\Omega = \Omega_1\Omega_2/\Delta$. When atoms are transferred from the up state to the down state in the Raman process, the momentum $\mathbf{q}_r = \mathbf{k}_1 - \mathbf{k}_2$ and energy $\hbar\Delta\omega = \hbar(\omega_2 - \omega_1)$ are transferred between photons and atoms. Considering the energy and momentum conservation in the Raman process, we obtain that

$$\hbar\Delta\omega = E_Z + \epsilon_{\uparrow}^{\text{initial}}(\mathbf{k}) - \epsilon_{\downarrow}^{\text{final}}(\mathbf{k}+\mathbf{q}_r), \tag{1}$$

where $\epsilon_{\uparrow}^{\text{initial}}(\mathbf{k})$ and $\epsilon_{\downarrow}^{\text{final}}(\mathbf{k}+\mathbf{q}_r)$ are energy-momentum dispersion of the spin up and down states, respectively, and E_Z is the energy split of the two hyperfine state. From Eq. (1), we can determine the energy-momentum dispersion of the initial state if the energy-momentum dispersion of the final state is known [for example, $\epsilon_{\downarrow}^{\text{final}}(\mathbf{k}) = \hbar^2\mathbf{k}^2/2m$ for the final state with the noninteraction]:

$$\epsilon_{\uparrow}^{\text{initial}}(\mathbf{k}) = \hbar\Delta\omega - E_Z + \epsilon_{\downarrow}^{\text{final}}(\mathbf{k}+\mathbf{q}_r). \tag{2}$$

If we consider the simplest case of the noninteraction fermion gas, i.e., the energy-momentum dispersions of the initial and

*jzhang74@yahoo.com, jzhang74@sxu.edu.cn

final states present the quadratic function with $\epsilon_\uparrow = \epsilon_\downarrow = \hbar^2\mathbf{k}^2/2m$, Eq. (1) becomes

$$\hbar\Delta\omega = E_Z - \frac{\hbar^2\mathbf{q}_r^2}{2m} - \frac{\hbar^2\mathbf{q}_r\cdot\mathbf{k}}{m}. \tag{3}$$

Since the parameters E_Z and $\mathbf{q}_r$ are fixed in experiment, the function between the frequency difference of two Raman beams and the atomic momentum is linear.

Next we analyze the RF spectrum. The RF transition is typically magnetic dipolar transition and the RF spectrum can probe the single-particle excitation spectrum, in which the momentum of the RF photon is effectively neglected. We have

$$\hbar\omega_{\rm RF} = E_Z + \epsilon_\uparrow^{\rm initial}(\mathbf{k}) - \epsilon_\downarrow^{\rm final}(\mathbf{k}). \tag{4}$$

From Eq. (4), the energy-momentum dispersion of the initial state can be determined when the energy-momentum dispersion of the final state is known,

$$\epsilon_\uparrow^{\rm initial}(\mathbf{k}) = \hbar\omega_{\rm RF} - E_Z + \epsilon_\downarrow^{\rm final}(\mathbf{k}). \tag{5}$$

Considering noninteracting fermions, the atoms in the hyperfine states ($|\uparrow\rangle$ and $|\downarrow\rangle$) will experience the same harmonic trap potential. Since the dispersions of the two states remain exactly parallel, the RF spectrum will present delta function $\hbar\omega_{\rm RF} = E_Z$.

The experimental setup has been described in our previous works [33–35]. The Bose-Fermi mixtures with ^{87}Rb at the spin state $|F=2,m_F=2\rangle$ and ^{40}K atoms at $|F=9/2,m_F=9/2\rangle$ are cooled in magnetic trap and then transported into an optical dipole trap. The Fermi gas in crossed optical trap with bosonic ^{87}Rb further is evaporatively cooled to $T/T_F \approx 0.3$ approximately 2×10^6 ^{40}K by reducing the powers of the laser beams, where T is the temperature, T_F is the Fermi temperature defined by $T_F = \frac{\hbar\overline{\omega}}{k_B}(6N)^{1/3}$, $\overline{\omega}$ is the trap mean frequency, and N is the number of fermions. When the Fermi gas reaches quantum degeneracy, the optical trap frequency is $2\pi\times(116,116,164)$ Hz along $(\hat{x},\hat{y},\hat{z})$ for ^{40}K. In order to remove the Rb atoms in the trap, we use a Rb resonant laser beam to shine the mixture in 0.03 ms without heating of ^{40}K atoms. A pair of bias magnetic coils are used to create a homogeneous magnetic field along $\hat{y}$ direction, which generates an energy split between hyperfine states $|F,m_F\rangle = |9/2,9/2\rangle$ and $|9/2,7/2\rangle$. In the optical trap, two spin states of ^{40}K atoms will experience the same trap potential.

For Raman spectroscopy, two $\lambda = 773$ nm laser beams counterpropagating along the $\hat{x}$ axis are linearly polarized along $\hat{y}$ and $\hat{z}$, respectively, which correspond to π and σ relative to quantization axis $\hat{y}$ [as shown in Figs. 1(a) and 1(b)]. Both beams are extracted from a Ti:sapphire laser operating at the wavelength of 773 nm with the narrow linewidth single-frequency and focused onto the central position of the optical trap with $1/e^2$ radii of 200 μm, which is larger than the atomic cloud size. Two Raman beams are frequency-shifted by single pass through two acousto-optic modulators (AOM) driven by two signal generators, respectively. The frequency difference of the two Raman lasers $\Delta\omega$ is adjusted by changing the frequency of the signal generator. We apply a Raman laser pulse with intensity $I = 50$ mW for each laser beam, and the duration time of 35 μs, which is much smaller than the optical trap period. After the Raman pulse, we immediately turn off the optical trap and the homogeneous magnetic field, let the

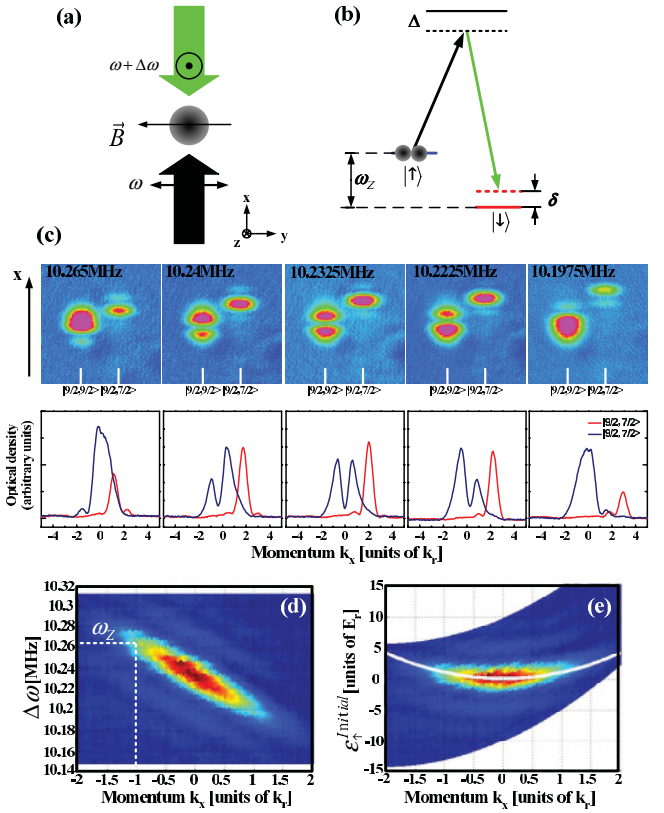

FIG. 1. (Color online) Experiment of Raman spectroscopy. (a) Schematic of the Raman spectroscopy. The two Raman beams counterpropagate along $\pm\hat{x}$ with frequency ω and $(\omega+\Delta\omega)$, linearly polarized along $\hat{y}$ and $\hat{z}$, correspond to π and σ relative to the quantization axis $-\hat{y}$. (b) The Raman transition with a Zeeman shift ω_Z and a detuning δ from the Raman resonance. (c) The absorption images of two hyperfine states after 12 ms TOF for different Raman frequency detuning. (d) Plot is intensity map of the atoms in the $|\downarrow\rangle$ state in the $(\Delta\omega,k_x)$ plane. (e) The translated intensity shows the atom number as a function of the single-particle energy (normalized to E_r) and momentum k_x (normalized to k_r). The white line is the expected quadratic dispersion curve.

atoms ballistically expand in 12 ms and take the time-of-flight (TOF) absorption image with a CCD (charge-coupled device). In order to measure the fraction of atoms in different hyperfine states, a gradient magnetic field along $\hat{y}$ direction is applied with 10 ms during the time of flight. The atoms in two spin states are spatially separated due to the Stern-Gerlach effect. The momentum transferred to atoms during the Raman process is $|\mathbf{q}_r| = 2k_r\sin(\theta)$, where $k_r = 2\pi/\lambda$ is the single-photon recoil momentum, λ is the wavelength of the Raman beam, and $\theta = 180^\circ$ is the intersecting angle of two Raman beams. Here, $\hbar k_r$ and $E_r = (\hbar k_r)^2/2m = h\times 8.34$ kHz are the units of momentum and energy.

All ^{40}K atoms are initially prepared in the $|F=9/2,m_F=9/2\rangle$ state (spin up state) and the final state $|F=9/2,m_F=7/2\rangle$ is empty. The homogeneous bias magnetic field is ramped to a certain value, which gives an energy split about $\omega_Z/2\pi \simeq 10.265$ MHz between hyperfine states $|F,m_F\rangle = |9/2,9/2\rangle$ and $|9/2,7/2\rangle$. Then we apply a Raman pulse with the duration of 35 μs to the gas, and measure the spin population for different frequency differences of the Raman lasers, as shown

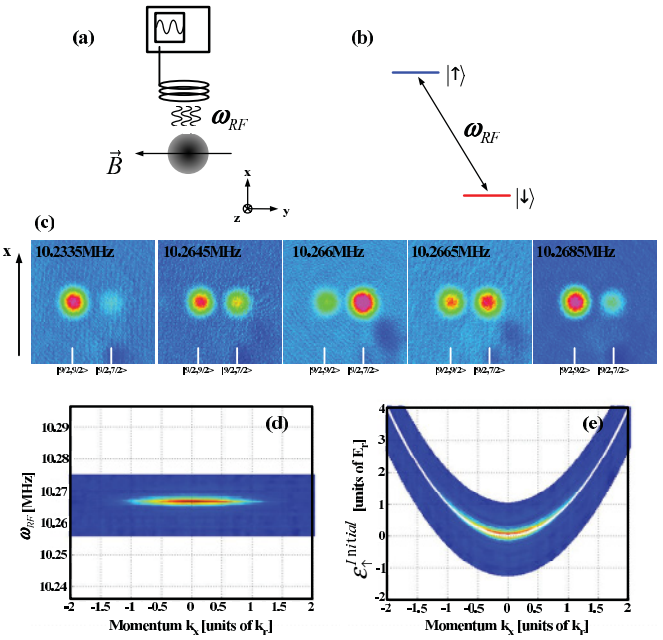

FIG. 2. (Color online) Experiment of RF spectroscopy. (a) Schematic of the RF spectroscopy experiment. The RF pulse is coupled to fermionic atoms with a quantization axis $-\hat{y}$ by a three loop coil. (b) Energy level for the atom-radiation interaction. (c) The absorption images of different hyperfine states after 12 ms TOF for different radio frequencies. (d) Plot is intensity map of the atoms in $|\downarrow\rangle$ state in the $(\omega_{\mathrm{RF}},k_x)$plane. (e) The translated intensity shows the atomic number as a function of the single-particle energy (normalized to E_r) and momentum k_x (normalized to k_r). The white line is the expected quadratic dispersion curve for the noninteracting Fermi gas.

in Fig. 1(c). We can see that only atoms in the certain momentum state are transferred from $|F=9/2,m_F=9/2\rangle$ to $|F=9/2,m_F=7/2\rangle$, which is determined by the frequency difference of the Raman lasers. It presents the inherent momentum-resolved characteristics of Raman spectroscopy. We integrate a TOF image along $\hat{y}$ to obtain the momentum distributions in $\hat{x}$ of two spin states, respectively, as shown in Fig. 1(c). The appearance of side lobes in the momentum distributions of the spin state $|9/2,7/2\rangle$ is due to the square envelope of Raman laser intensity. Then all momentum distributions in axis $\hat{x}$ of the spin state $|9/2,7/2\rangle$ for different frequency differences of the Raman lasers are plotted in the $(\Delta\omega,k_x)$ plane, as shown in Fig. 1(d), where all momentum distributions in axis $\hat{x}$ have been translated for the two-unit momentum $-\mathbf{q}_r=-2k_r$. The distribution of Fig. 1(d) clearly shows the linear relationship [see Eq. (3)] between the atomic momentum and the frequency difference of two Raman beams for noninteraction Fermi gas. According to Eq. (2) and the quadratic energy-momentum dispersion of the final state, the energy-momentum dispersion of the initial state $|9/2,9/2\rangle$ [Fig. 1(e)] is obtained from the measured spectrum [Fig. 1(d)]. Figure 1(e) shows the distribution of the atom number in the initial spin state as a function of the single-particle energy and momentum, which is in good agreement with the expected behavior of the quadratic function.

We also carry out the RF spectroscopy in order to compare with the Raman spectroscopy, which are shown in Figs. 2(a) and 2(b). A Gaussian shape pulse of RF is applied to transfer atoms from the initial state $|9/2,9/2\rangle$ to the final state $|9/2,7/2\rangle$. The RF radiation is produced by function generator (SRS DS345), and is controlled by a voltage-controlled RF attenuator for generating Gaussian shape pulse. The RF pulse is amplified by a power amplifier (Mini-circuit ZHL-5W-1), then delivered to the atomic cloud by a simple three-loop coil. The RF Gaussian envelope hence results in the elimination of the side lobes. With the same homogeneous magnetic field, we apply a RF Gaussian pulse for 200 μs and measure the spin population for different RF frequencies, as shown in Fig. 2(c). At the resonance frequency, almost all atoms are transferred to the $|9/2,7/2\rangle$ state, no matter how much the momentum of atoms is. The larger the detuning from the resonance frequency is, the smaller the number of transferred atoms is. The width of the RF response is about 3 kHz. We integrate TOF image along $\hat{y}$ to obtain the momentum distributions in $\hat{x}$ of the spin state $|9/2,7/2\rangle$, then arrange all curves for the different frequencies of RF pulse into the (ω_{RF},k_x) plane, as shown in Fig. 2(d). The distribution of Fig. 2(d) shows the delta function. The energy-momentum dispersion of the initial state $|9/2,9/2\rangle$ [Fig. 2(e)] can also be obtained from the measured spectrum [Fig. 2(d)] using Eq. (5), which is in good agreement with that measured by the Raman spectroscopy.

In conclusion, we have demonstrated the momentum-resolved Raman spectroscopy technology experimentally, which is in analogy to the angle-resolved photoemission spectroscopy of solid state physics. The single-particle property is probed and the dispersion in an ultracold noninteracting Fermi gas is measured. The experiment results are in good agreement with that obtained with RF spectroscopy technology. Momentum-resolved Raman spectroscopy technology can be used to study the single-particle state in BEC-BCS crossover, and some effects of final states or molecular states, especially if its spatial selectivity is utilized.

This research is supported by National Basic Research Program of China (Grant No. 2011CB921601), NSFC Project for Excellent Research Team (Grant No. 61121064), and Doctoral Program Foundation of Ministry of Education China (Grant No. 20111401130001).

[1] M. Greiner, C. A. Regal, and D. S. Jin, Nature (London) **426**, 537 (2003).

[2] S. Jochim, M. Bartenstein, A. Altmeyer, G. Hendl, S. Riedl, C. Chin, J. Hecker Denschlag, and R. Grimm, Science **302**, 2101 (2003).

[3] M. W. Zwierlein, C. A. Stan, C. H. Schunck, S. M. F. Raupach, S. Gupta, Z. Hadzibabic, and W. Ketterle, Phys. Rev. Lett. **91**, 250401 (2003).

[4] C. Chin, M. Bartenstein, A. Altmeyer, S. Riedl, S. Jochim, J. Hecker Denschlag, and R. Grimm, Science **305**, 1128 (2004).

[5] J. T. Stewart, J. P. Gaebler, and D. S. Jin, Nature (London) **454**, 744 (2008).
[6] G. Jo, Y. Lee, J. Choi, C. A. Christensen, T. H. Kim, J. H. Thywissen, D. E. Pritchard, and W. Ketterle, Science **325**, 1521 (2009).
[7] J. Simon, W. S. Bakr, R. Ma, M. E. Tai, P. M. Preiss, and M. Greiner, Nature (London) **472**, 307 (2011).
[8] Y.-J. Lin, R. L. Compton, K. Jiménez-García, J. V. Porto, and I. B. Spielman, Nature (London) **462**, 628 (2009).
[9] Y.-J. Lin, K. Jiménez-García, and I. B. Spielman, Nature (London) **471**, 83 (2011).
[10] Z. Fu, P. Wang, S. Chai, L. Huang, and J. Zhang, Phys. Rev. A **84**, 043609 (2011).
[11] S. Chen, J. Y. Zhang, S. C. Ji, Z. Chen, L. Zhang, Z. D. Du, Y. J. Deng, H. Zhai, and J. W. Pan, e-print arXiv:1201.6018.
[12] P. Wang, Z. Yu, Z. Fu, J. Miao, L. Huang, S. Chai, H. Zhai, and J. Zhang, e-print arXiv:1204.1887.
[13] *Proceedingsof the International School of Physics Enrico Fermi (Course CLXIV)*, edited by M. Inguscio, W. Ketterle, and C. Salomon (IOS Press, Amsterdam, 2006).
[14] S. Nascimbène, N. Navon, K. J. Jiang, F. Chevy, and C. Salomon, Nature (London) **463**, 1057 (2010).
[15] R. G. Scott, F. Dalfovo, L. P. Pitaevskii, and S. Stringari, Phys. Rev. Lett. **106**, 185301 (2011).
[16] E. Altman, E. Demler, and M. D. Lukin, Phys. Rev. A **70**, 013603 (2004).
[17] C. A. Regal and D. S. Jin, Phys. Rev. Lett. **90**, 230404 (2003).
[18] S. Gupta, Z. Hadzibabic, M. W. Zwierlein, C. A. Stan, K. Dieckmann, C. H. Schunck, E. G. M. van Kempen, B. J. Verhaar, and W. Ketterle, Science **300**, 1723 (2003).
[19] Y. Shin, C. H. Schunck, A. Schirotzek, and W. Ketterle, Phys. Rev. Lett. **99**, 090403 (2007).
[20] Q. Chen and K. Levin, Phys. Rev. Lett. **102**, 190402 (2009).
[21] Q. Chen, Y. He, C. Chien, and K. Levin, Rep. Prog. Phys. **72**, 122501 (2009).
[22] T.-L. Dao, A. Georges, J. Dalibard, C. Salomon, and I. Carusotto, Phys. Rev. Lett. **98**, 240402 (2007).
[23] T.-L. Dao, I. Carusotto, and A. Georges, Phys. Rev. A **80**, 023627 (2009).
[24] G. Veeravalli, E. Kuhnle, P. Dyke, and C. J. Vale, Phys. Rev. Lett. **101**, 250403 (2008).
[25] E. D. Kuhnle, S. Hoinka, P. Dyke, H. Hu, P. Hannaford, and C. J. Vale, Phys. Rev. Lett. **106**, 170402 (2011).
[26] B. Fröhlich, M. Feld, E. Vogt, M. Koschorreck, W. Zwerger, and M. Köhl, Phys. Rev. Lett. **106**, 105301 (2011).
[27] M. Feld, B. Fröhlich, E. Vogt, M. Koschorreck, and M. Köhl, Nature (London) **480**, 75 (2011).
[28] A. T. Sommer, L. W. Cheuk, M. J. H. Ku, W. S. Bakr, and M. W. Zwierlein, Phys. Rev. Lett. **108**, 045302 (2012).
[29] Y. Zhang, W. Ong, I. Arakelyan, and J. E. Thomas, e-print arXiv:1201.3560.
[30] S. Konabe, T. Nikuni, and M. Nakamura, Phys. Rev. A **73**, 033621 (2006).
[31] P. B. Blakie, New J. Phys. **8**, 157 (2006).
[32] G. Tackmann, B. Pelle, A. Hilico, Q. Beaufils, and F. Pereira dos Santos, Phys. Rev. A **84**, 063422 (2011).
[33] D. Xiong, H. Chen, P. Wang, X. Yu, F. Gao, and J. Zhang, Chin. Phys. Lett. **25**, 843 (2008).
[34] D. Xiong, P. Wang, Z. Fu, and J. Zhang, Opt. Express **18**, 1649 (2010).
[35] P. Wang, L. Deng, E. W. Hagley, Z. Fu, S. Chai, and J. Zhang, Phys. Rev. Lett. **106**, 210401 (2011).